Automated Kaguya TC and MRO CTX Stereo DEM Generation. L. A. Adoram-Kershner[1], B. H. Wheeler[1], J. R. Laura[1], and R. L. Fergason[1], D. P. Mayer[1], [1]USGS Astrogeology 2255 N. Gemini Dr. Flagstaff, AZ 86001; ladoram-kershner@usgs.gov

Introduction: Digital Elevation Models (DEMs) are foundational products within a Planetary Spatial Data Infrastructure (PSDI) [1,2] and support a myriad of science and engineering applications [e.g.,3,4]. DEMs can be produced by applying stereogrammetry concepts to stereographic images (termed stereopairs). Due to the expertise and time required to generate DEMs, stereopairs for Mars and the Moon are frequently acquired at a faster rate than DEMs. Currently, individual research scientists must either obtain the tools and training to independently conduct stereogrammetry or obtain completed products from mission teams or research groups that have publicly released these products. Herein, we describe the automated generation, validation, and publication of DEMs using the USGS Integrated Software for Imagers and Spectrometers (ISIS) [5] and the NASA Ames Stereo Pipeline (ASP) [6]. Our pipeline starts with raw image data, preprocesses and calibrates it, and generates DEMs with minimal human involvement. The pipeline is currently being applied to the Mars Reconnaissance Orbiter Context Camera (CTX) [7] and Kaguya Terrain Camera (TC) [8] data. This work builds on previous research conducted by Mayer et al. concerning automatic generation of DEMs [9,10].

Image Processing: The pipeline begins with raw image data, so that DEMs can be generated with updated data, calibration or processing improvements from mission teams. Initial image processing is completed using ISIS ingestion (*mroctx2isis* or *kagtc2isis*), *spiceinit*, and the available mission specific ISIS commands. For CTX these mission specific commands include *ctxcal* and *ctxevenodd* (as needed). Kaguya TC has no mission specific calibration commands in ISIS as of version 4.2.0, thus so *spiceinit* was the only preprocessing performed.

DEM Generation: Once the ISIS cubes are ingested and preprocessed, ASP is used for DEM generation. First ASP's *bundle_adjust* is used to relatively align the stereo images through camera orientation adjustments. Then the bulk of the DEM generation is accomplished with *parallel_stereo*. The pipeline leverages *parallel_stereo* steps 0, 1, 3, 4, and 5 corresponding to preprocessing (stereo_pprc), disparity map initialization (stereo_corr), subpixel refinement(stereo_rfne), outlier rejection and hole filling (stereo_fltr), and triangulation (stereo_tri). The parameterization of these steps is provided in Table 1.

Table 1: Parameterization of *parallel_stereo* steps.

Function (Step)	Argument	Values
stereo_pprc (0)	alignment-method	affineepipolar
	prefilter-mode	2 (Laplacian of Gaussian)
	prefilter-kernel-width	1.5
stereo_corr (1)	stereo-algorithm	0 (block matching)
	corr-seed-mode	1 (low-res disparity from stereo)
	cost-mode	2 (normalized cross correlation)
	corr-kernel	27 27
stereo_rfne (3)	subpixel-mode	2 (bayes EM weighting)
	subpixel-kernel	21 21
stereo_fltr (4)	rm-cleanup-passes	0
	median-filter-size	7
	texture-smooth-size	13
	texture-smooth-scale	0.13
stereo_tri (5)	compute-error-vector	true

Currently the CTX and Kaguya TC pipelines use the same stereo configuration. The parameterization was developed by Mayer through parameter sweeps on CTX data [10]. Applying these parameters on the Kaguya TC data produces reasonable DEMs; however, future work includes conducting a parameter sweep for the Kaguya TC data to further improve the results.

A point cloud is generated using *parallel_stereo* and the relatively aligned stereo pairs. To enforce a relationship to ground an Iterative Closest Point method (ICP), using the application *pc_align*, aligns the *parallel_stereo* point cloud with a point cloud acquired from ground laser altimetry data. The results of *pc_align* are more accurate when the input point clouds are in approximate alignment before the ICP method is applied. Therefore, the point cloud is compared to the ground altimetry data using *geodiff* to find the average offset. For CTX and Kaguya TC data, this offset is typically largest in the vertical direction, so the difference is applied as an initial downward translation (*pc_align* --initial-ned-translation 0 0 X).

The DEM products are created from the ground-controlled point cloud and *point2dem* using an orthographic projection centered on the DEM's centroid. The DEM grid spacing for CTX is 20 meters/pixel and Kaguya TC is 35 meters/pixel to work with approximate data resolutions of 7 meters/pixel and 10 meters/pixel, respectively.

Ground sources. The accepted geodetic reference frame for Mars is the Mars Orbiter Laser Altimeter (MOLA) [11] data set. The accepted geodetic reference frame for the Moon is Lunar Orbiter Laser Altimeter (LOLA) obtained from the Orbital Data Explorer (ODE) [12]. In both cases the ground source data is being queried with a tight footprint and only includes ground points that fall within the DEM footprint.

Validation Process: We validated our pipeline by comparing our CTX stereo DEMs to DEMs hand-generated in SOCET SET® and the MOLA-MEX HRSC Blended Global DEM [13]. The SOCET SET® generated DEMs were created as part of the candidate Mars 2020 landing site analyses and have a grid spacing of ~20 meters [14], whereas the MOLA-MEX HRSC Blended Global DEM is considered a community standard for Mars ground with a grid spacing of ~200 meters. Figure 1 shows the histogram of the elevation differences between the ASP generated DEM and the two benchmark DEMs at an area focused on the Martian feature Northeast Syrtis.

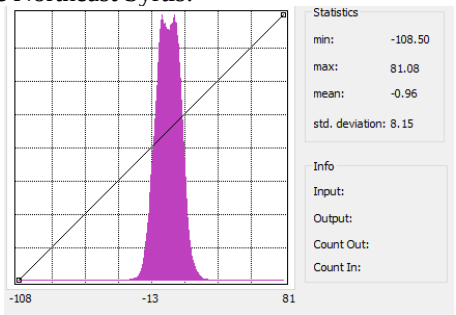

(a)

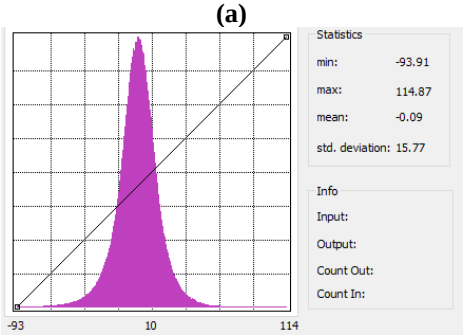

(b)

Figure 1: Histogram of elevation differences at Northeast Syrtis between the DEM generated in ASP and (a) DEM generated with SOCET SET® (b) MOLA-MEX HRSC Blended Global DEM

Preliminary inspection of the elevation differences shows broad agreement with the means and standard deviations well within the precision of the products' resolutions. Further benchmark validation comparisons for both CTX and Kaguya TC data sets are under investigation by the team.

A validation step is also in the pipeline and can be viewed for every DEM. After aligning the point cloud to the ground laser altimetry data with *pc_align*, *geodiff* is run again to calculate the difference from the ground-controlled point cloud to the ground laser altimetry data. The distribution of these differences is packaged with the public release of the data in a file called qa_metrics.txt.

Data Serving: The usefulness of these products is dependent on their discoverability, interoperability, and reproducibility as described by the FAIR guiding principles framework (https://www.go-fair.org/fair-principles/). To that end, we are serving the DEMs and their associated orthoimages as analysis ready data (ARD), using the spatio-temporal asset catalog (STAC) [15]. These data are served as cloud optimized geotiffs (COGs) which are analysis and GIS ready without additional processing. We also serve FGDC compliant metadata [16] and provenance files (a history of processing steps used to produce the DEMs) to further improve reproducibility. After validation, we will make all data publicly available via Amazon Web Service (AWS) S3 buckets.

Acknowledgments: The MRO CTX data were provided by the PDS Cartography and Imaging Sciences Node. The MOLA and LOLA data were provided by the PDS Geosciences Node. Kaguya TC data and support were provided by the SELENE team and Data Archive operated by JAXA. Any use of trade, firm, or product names is for descriptive purposes only and does not imply endorsement by the U.S. Government.

References: [1] Gaddis L. (2018) *LPSC XLIX*, 2081 or 1540. [2] Laura J. R., et al. (2017) *ISPRS International Journal of Geo-Information* 6.6, 181. [3] Kirk, R. L., et al. (2008) J. Geophys. Res., 113, E00A24, doi:10.1029/2007 JE003000. [4] Xiong, S., et al. (2021) *Earth and Space Science*, 8(1), e2019EA000968. [5] USGS Astrogeology (2020) https://doi.org/10.5281/zenodo.3962369. [6] Beyer et al. (2020) https://doi.org/10.5281/zenodo.396334. [7] Malin, M. C., et al. (2007) *J. Geophys. Res.*,112, E05S04, doi:10.1029/2006JE002808. [8] Haruyama, J., Matsunaga, T., Ohtake, M. et al. (2008) *Earth Planet Space* 60, 243–255, doi:10.1186/BF03352788. [9] Mayer, D.P. and Kite, E.S. (2016) *LPS XLVII*, ePosterAbstract No. 1241. [10] Mayer, D.P. (2018) *LPSC XLIX*, Abstract No. 1604. [11] Neumann, G. A, et al. (2001) *J. Geophys. Res.*, 106, 23,753–23,768. [12] Smith, D. E., et al. (2008) *Eos Trans. AGU*, 87 (52), U41C – 0826. [13] Fergason, R. L, Hare, et al. (2018) *Astrogeology PDS Annex*. http://bit.ly/HRSC_MOLA_Blend_v0 [14] Fergason R. L., et al. (2017) *LPSC XLVIII*, No. 1964, id.2163. [15] SpatioTemporal Asset Catalog. (2019) *SpatioTemporal Asset Catalog*, [Online] https://radiantearth. github.io/stac-site/. [16] Federal Geographic Data Committee. (1998) *Federal Geographic Data Committee*, FGDC-STD-001-1998.